Radiatively Improved Mode in a Tokamak: a theoretical model

R. Singh 1), P. K. Kaw 1), A. Rogister 2) and V. Tangri 1)

1) Institute for Plasma Research, Gandhinagar – 382 428, India

2) Institute for Plasma Physics, Forschungszentrum Juelich,

D-52425 Juelich, Germany

e-mail contact of main author: rsingh@ipr.res.in & rsingh129@yahoo.co.in

Abstract. It is well known from impurity seeding experiments in several limiter tokamaks that the plasma may bifurcate into an improved confinement mode, the so called RI mode. In this mode, the confinement improvement is associated with density and temperature peaking and stronger velocity shear. In this paper we propose a novel model for the RI mode. It is demonstrated that radiative effects from impurities distributed in a poloidally asymmetric manner lead to significant density and temperature perturbations on magnetic surfaces. These, in turn, interact with theta dependent toroidal field variations to produce a mean divergence of the stress tensor driving strong toroidal flows. The resulting enhanced toroidal velocity shear on the outer radiative layers produces a stabilizing effect on the instabilities like the drift resistive ballooning mode, drift trapped electron mode and the ion temperature gradient mode. By an investigation of the turbulent particle flux as a function of the density gradient for various values of the radiation asymmetry parameter, it is shown that the plasma can undergo a bifurcation into a better- confined peaked density state.

1. Introduction

The Radiative improved (RI) mode, the improved confinement mode for limiter tokamaks arising due to injection of impurities like Neon, Argon etc. This confinement mode was discovered originally in the ISX-B tokamak [1,2]. Later it was thoroughly reinvestigated in the pioneering research on the TEXTOR-94 tokamak [3-6]. The RI mode is characterized by more peaked density, temperature and toroidal velocity shear profiles, peak densities well above the Greenwald density limit, confinement times close to the ELMy H- mode values and a density scaling like the neo-Alcator scaling.

The present models of improved confinement in the RI mode are largely based on a reduction of the growth characteristics of the toroidal ion temperature gradient (ITG) mode, when the plasma Z_{eff} increases [7]. Experimentally there is evidence [8] that the $\vec{E}\times\vec{B}$ shear rotation in the impurity-injected plasma is much stronger than in the normal plasma, yet there seems to be little effort either to explain this feature or to use it to stabilize the ITG mode. In all likelihood, both effects are taking place, namely a direct reduction of the ITG growth rate due to increase of Z_{eff} and a suppression of the turbulence due to the increased velocity shear of these discharges.

This paper is devoted to exploring the mechanisms associated with impurity injection, which may influence the $\vec{E}\times\vec{B}$ velocity shear profile. The mechanism that we propose is directly related to impurity injection. When an impurity like Neon is injected in typical L - Mode plasma, it radiates copiously till it reaches the Lithium and Beryllium like states. This typically

happens in the outer $20\% - 25\%$ of the discharge radius. The impurities are typically not distributed symmetrically in the poloidal direction but show in – out and up – down asymmetries [3]. Quantitatively, the asymmetry in concentration could be as much as a factor of two. This leads to strong poloidal asymmetries in the radiation from the plasma even in a regime where the MARFE is absent (i.e., in the thermally stable regime when the power lost by impurity radiation is well below the input power). An asymmetrically radiating plasma produces temperature and density perturbations on the magnetic surface that interact with the theta dependent toroidal field variations to produce a mean divergence of the stress tensor which drives significant toroidal flows on these surfaces. An important feature of these flows is that they have significant magnitude and exist only in the radiative region. This then has the effect of producing a significantly enhanced toroidal velocity shear ($U_{\phi,i}^{/}$) (where prime denotes differentiation in r) near the radiative layer. This, in turn, leads to an increase of the radial electric field strength through the radial force balance equation $E_r / B_\phi = (T_i / e)\partial \ln P_i / \partial r + (B_\theta / B_\phi)U_{\phi i} - U_{\theta i}$. That is then responsible for an increase in the $\vec{E}\times\vec{B}$ rotation velocity shear $< U_E >^{/} = < U_{\theta,i} >^{/} - (\varepsilon / q) < U_{\phi,i} >^{/} - (4\varepsilon_i^{\,2}\rho_i c_i / R^2)p(1-p)$ (where $p = L_{T_i} / L_N = \eta_i^{-1}$ is the peaking factor, $U_{\theta,i} \approx -1.83(T_i / eB_\phi)(\partial \ln T_i / \partial r)$ is the poloidal ion velocity in Pfirsh-Schlüter regime [9-10]). Now it is well known that $\vec{E}\times\vec{B}$ shear rotation can suppress the tokamak background turbulence. Furthermore, a consensus is emerging around the view that the turbulence processes in the radiative outer region of a tokamak are dominated by the ion temperature gradient (ITG) instability [11], the dissipative trapped electron mode (DTE)) [12,13], and high-m drift resistive ballooning mode (DRBM) [14]. We thus expect the radiation asymmetry driven $\vec{E}\times\vec{B}$ shear flows to suppress these instabilities in the radiative edge plasma. This leads to a reduction in particle and thermal convective fluxes which locally sharpens the density and temperature profiles. If this sharpening of the profiles leads to further suppression of the turbulence, the plasma may bifurcate into a better confined and highly peaked density profile state.

2. Basic Equations

We start from Braginskii's two fluid equations including the Mikhailovskii and Tsypin corrections of the stress tensor. These equations are

$$\frac{\partial N_i}{\partial t} + \vec{\nabla}\cdot N_i\vec{U}_i = 0 \tag{5}$$

$$m_i N_i(\frac{\partial}{\partial t} + \vec{U}_i\cdot\vec{\nabla})\vec{U}_i = -\vec{\nabla}P_i - \vec{\nabla}\cdot\vec{\pi}_i + eN_i(\vec{E} + \vec{U}_i\times\vec{B}) \tag{6}$$

$$\frac{3}{2}N_i(\frac{\partial}{\partial t} + \vec{U}_i\cdot\vec{\nabla})T_i + P_i\vec{\nabla}\cdot\vec{U}_i = -\vec{\nabla}\cdot\vec{q}_i \tag{7}$$

where Eqs. (5) – (7) are the ion continuity, momentum and energy equations, respectively, $\vec{p}_i$ is the ion stress tensor given by Braginskii [15] and Mikhailovskii and Tsypin[17], $\vec{q}_i = -k_{//i}\nabla_{//}T_i - k_{\perp i}\nabla_\perp T_i + k_{xi}\hat{n}\times\vec{\nabla}T_i$ is the diffusive ion thermal flux, $k_{//i} = 3.9(N_i T_i / m_i n_i)$

and $\kappa_{\perp i}$ are the parallel and perpendicular diffusion coefficient, respectively and $k_{xi} = 5N_iT_i / 2m_i\Omega_i$; other notations are standard.

We assume the poloidal variation of the radiation power density (Q_{rad}) is of the form $Q_{rad} = Q_{rad}^{(0)}[1+\Delta_1\cos(q-q^*)]$, where q is the poloidal angle, $q=0$ denotes the low field side mid-plane, q^* is the location of the maximum radiation, and Δ_1 is the degree of asymmetry. In the limit, $(\Omega_e/n_{e,i})(rL_{T_e}/q^2R^2) > 1$ (i.e., parallel electron thermal conduction dominant over convection processes), the poloidally asymmetric electron temperature perturbation is given by steady-state heat balance equation,

$$\vec{\nabla}\cdot\vec{q}_e = -Q_{rad}^{(0)}(r)[1+\Delta_1\cos(q-q^*)] + H(r), \tag{8}$$

where $\vec{q}_e = -k_{\perp,e}\nabla_\perp T_e - k_{//,e}\nabla_{//}T_e$ is the total heat flux, $k_{\perp,e}(k_{//,e})$ is the perpendicular (parallel) electron thermal conductivity [15], $k_{//,e} = 3.2N_eT_e/m_en_e$, $\kappa_{\perp e}$ is determined by anomalous processes and $H(r)$ is the local plasma heating rate.

The generalized co-ordinate system ($\hat{p},\hat{b},\hat{n}$) is used, which is tied to magnetic field. Here $\hat{n} = \vec{B}/B$ is the unit vector along the magnetic field lines, $\hat{p}$ is the orthogonal to the magnetic surface, and $\hat{b} = \hat{n}\times\hat{p}$. The unit vectors $\hat{p},\hat{b},\hat{n}$ are related to the flux co-ordinates $\hat{e}_y, \hat{e}_c, \hat{e}_f$ (where y is the poloidal magnetic flux, c the generalized poloidal angle and f is the toroidal angle) by

$$\hat{p} = \hat{e}_\psi, \quad \hat{b} = \left(\frac{B_\phi}{B}\right)\hat{e}_\chi - \left(\frac{B_\chi}{B}\right)\hat{e}_\phi, \quad \hat{n} = \left(\frac{B_\chi}{B}\right)\hat{e}_\chi + \left(\frac{B_\phi}{B}\right. \tag{9}$$

where $h_\psi = 1/h_\phi B_\chi, h_\chi = JB_\chi$, $J = h_\psi h_\chi h_\phi$ is the Jacobian of the transformation ($\vec{r}\to\psi,\chi,\phi$), $\nu = h_\chi B_\phi / h_\phi B_\chi \sim rB_\phi/RB_\chi$ is the pitch of the field lines, $q = \oint \nu\, d\chi$ is the safety factor. We note that $h_\phi = R_0(1+\varepsilon\cos\chi), B_\phi = B_{\phi 0}(1-\varepsilon\cos\chi)$ and $\chi\sim\theta$ in case of large aspect ratio tokamak with circular cross section, where $\varepsilon = r/R_0$ is the inverse aspect ratio, r, and R_0 the minor and major radii, respectively. We consider the scaling relevant to the edge of tokamaks edge

$$\frac{r}{qR} \sim \frac{c_i}{qR\nu_i} \sim \frac{L_\psi}{r} \sim \left(\frac{m_e}{m_i}\right)^{1/4} \sim \left(\frac{a_i}{L_\psi}\right)^{1/2} \sim \mu << 1, \tag{10}$$

and

$$\nu_{cx} \sim \nu_{ion} \le \nu_i; \qquad L_\psi \sim L_{N,T} \tag{11}$$

where ν_i is the ion collision frequency, $L_\psi \sim L_{N,T}$ the plasma density or temperature gradient scale, $m_i(m_e)$ the ion (electron) mass, $c_i = \sqrt{T_i/m_i}$ the ion thermal velocity, $a_i = c_i/\Omega_i$ the ion Larmor radius, $\Omega_i = eB/m_i$ the ion cyclotron frequency, and μ the small expansion parameter.

3. Neoclassical Toroidal Flow

Summing up the toroidal component of the ion and electron momentum equations yields the radial current density

$$J_{\psi} = \frac{1}{B_{\chi}} \hat{e}_{\phi} \cdot [\vec{\nabla} \cdot \vec{\pi}_i + m_i N_i (\frac{\partial}{\partial t} + \vec{U}_i \cdot \vec{\nabla}) \vec{U}_i + M_{cx}(\psi, \chi) \tag{12}$$

Combining Eqs. (5) and (12) and integrating the resulting expression over magnetic flux surfaces leads to the relation

$$\begin{aligned} \oint J_{\psi} h_{\chi} h_{\phi} \frac{d\chi}{2\pi} &= \oint J h_{\phi} \frac{d\chi}{2\pi} [\frac{\partial (m_i N_i U_{\phi i})}{\partial t} \\ &+ \oint \hat{e}_{\phi} \cdot (\vec{\nabla} \cdot \vec{\pi}_i) J h_{\phi} \frac{d\chi}{2\pi} + \frac{\partial}{\partial \psi} \oint J h_{\phi} h_{\psi}^{-1} m_i N_i U_{\psi i} U_{\phi i} \frac{d\chi}{2\pi} \end{aligned} \tag{13}$$

We neglect the momentum flux driven by background turbulence, toroidal momentum transfer due to neoclassical radial convection effects and the standard charge exchange damping with neutrals due to recycling from wall. The averaged over magnetic flux surfaces, the stationary (i.e. $\partial / \partial t \to 0$) equation for $U_{\phi i}^{(0)}$ may be written as

$$\oint \hat{e}_{\phi} \cdot (\vec{\nabla} \cdot \vec{\pi}_i) J h_{\phi} \frac{d\chi}{2\pi} = 0 \tag{14}$$

The contribution from the off diagonal tensor can be written in leading order as

$$\begin{aligned} &\oint \hat{e}_f \cdot (\vec{\nabla} \cdot \vec{p}_i) J h_f \, dc \\ &= \frac{\partial}{\partial y} \oint h_y^{-1} J h_f \, dc \, (p_{3-4,i})_{yf} + \frac{\partial}{\partial y} \oint h_y^{-1} J h_f \, dc \, [(p_{1-2,i})_{yf} \\ &= -\frac{m_i}{e} \frac{\partial}{\partial y} \{ h_f^{\,2} B_f^{\,2} \oint dc \, [\frac{P_i}{B^4} \frac{\partial}{\partial c} (U_{//i} B) + \frac{8}{5} \frac{q_{//i}}{B^4} \frac{\partial B}{\partial c}] \} \\ &\qquad - \frac{12}{10} \frac{m_i}{e} \frac{\partial}{\partial y} \{ h_f^{\,2} B_f^{\,2} \oint dc \, [\frac{n_i}{\Omega_i} \frac{B_c J}{B_f} \frac{P_i}{B^2} h_y^{-1} \frac{\partial U_{//i}}{\partial y}] \} \end{aligned} \tag{15}$$

For $U_{fi} \sim m c_i$, $U_{ci} \sim m^2 c_i$, $U_{yi} \approx 0$, the Eq. (15) can be rewritten as

$$\begin{aligned} &\frac{\partial}{\partial \psi} \{ \frac{P_i^{(0)}}{B_0^{\,3}} \oint [(p_i^{(1)} - 4b^{(1)}) (\frac{\partial u_{//i}^{(1)}}{\partial \chi} + U_{//i}^{(0)} \frac{\partial b^{(1)}}{\partial \chi}) \\ &- 1.6 \chi_{//i}^{(0)} \frac{B_{\chi}^{(0)}}{B_0} \frac{1}{h_{\chi}^{(0)}} (\frac{\partial t_i^{(1)}}{\partial \chi} \frac{\partial b^{(1)}}{\partial \chi})] \frac{d\chi}{2\pi} + \frac{12}{10} \frac{P_i^{(0)}}{B_0^{\,2}} \frac{\nu_i^{(0)}}{\Omega_i^{(0)}} \frac{h_{\chi}^{(0)}}{B_{\phi 0}} \frac{1}{h_{\psi}^{(0)}} \frac{\partial U_{//i}^{(0)}}{\partial \psi} \} = 0 \end{aligned} \tag{16}$$

where $p_i^{(1)} = p_j / P_j^{(0)}$, $n_j^{(1)} = n_j / N_j^{(0)}$, $t_j^{(1)} = t_j / T_j^{(0)}$ and $f^{(1)} = ef / T_e^{(0)}$ are the normalized perturbed variables. For $\Delta_1 \sim m << 1$, the poloidal variation of the electron temperature due to asymmetric radiation in an equilibrium state can be obtained from steady-state heat balance equation. The solution is

$$t_e^{(1)} = -d^{(0)} \cos(q - q^*), \tag{17}$$

where $d^{(0)}(r) = Q_{rad}^{(0)} \Delta_1 q^2 R^2 / T_e^{(0)} k_{//,e}^{(0)}$. In the large mobility limit ($m_e / m_i \to 0$), the theta dependent electron temperature perturbation combines with the parallel electron momentum equation in the leading order (i.e., $eN_e E_{//} + \nabla_{//} P_e + 0.71 N_e \nabla_{//} T_e = 0$) and results in a modified electron adiabatic relation given by

$$t_i f^{(1)} = n^{(1)} - 1.17 d^{(0)} \cos(q - q^*), \tag{18}$$

\

where $t_i = T_i / T_e$, $n_i^{(1)} \sim n_e^{(1)} \sim n^{(1)}$ (quasi-neutral condition). Similarly the parallel ion momentum equation to leading order results in

$$t_i^{(1)} = -(1 + 1/\tau_i) n + 1.71 (\delta^{(0)} / \tau_i) \cos(\theta - \theta^*), \tag{19}$$

Combining Eqs. (16) – (19), the stationary equation for $U_{f,i}^{(0)}$ is then written as

$$\begin{aligned} \frac{\partial U_{\phi,i}}{\partial r} = & -0.8 \frac{q^3 \varepsilon_i^2}{\varepsilon} \frac{\rho_i c_i}{R^2} [1 - 40.7 (1 + \frac{0.94}{\eta_i} + \frac{0.22}{\eta_i^2}) \frac{\delta^{(0)}}{\varepsilon} \cos\theta^*] \\ & + 4.45 (\frac{c_i^2 \Omega_i}{R^2 \nu_i^2}) \frac{\delta^{(0)}}{q} (\cos\theta^* - \sin\theta^*) - 1.2 (1 - \frac{0.96}{\eta_i}) \frac{q \varepsilon_i}{\varepsilon^2} \frac{\rho_i c_i}{R^2} \frac{\Omega_i}{\nu_i} \delta^{(0)} \varepsilon \sin\theta^* \end{aligned} \tag{20}$$

where $\varepsilon_i = R(-\partial \ln T_i / 2\partial r) = R / 2L_{T_i}$. Note that in the absence of asymmetric radiation, we recover the results of Classen *et al* [10] for the toroidal flow. Among the radiation asymmetry driven terms the dominant contribution to toroidal velocity shear comes from the second term of Eq.(20) which is multiplied by 4.45. The physical origin for this term is a component of the divergence of the stress tensor proportional to $-1.6 (\chi_{//i}^{(0)} B_\chi^{(0)} / B_0 h_\chi^{(0)}) \oint (\partial t_i^{(1)} / \partial \chi)(\partial b^{(1)} / \partial \chi) d\chi / 2\pi$. Note that $t_i^{(1)} \sim t_e^{(1)} \sim \delta^{(0)}$, where $\delta^{(0)}$ is related to the radiation asymmetry parameter Δ_1. In terms of order of magnitude $\delta^{(0)} \sim Q_{rad}^{(0)} \Delta_1 q^2 R^2 / T_e^{(0)} \kappa_{//,e}^{(0)} \sim (P_{e0}^{core} \Delta_1 / P_{e0}^{edge} \nu_{ei} \tau_E)(qR / \lambda_f)^2$; τ_E is the energy confinement time and λ_f is the electron mean free path .

We now apply our results to the experimental observations of RI mode in typical TEXTOR-94 discharges [3,4,5,6]. In RI-mode, the TEXTOR-94 edge parameters are: $T_i^{(0)} = 150eV$, $T_e^{(0)} = 80eV$, $N_i^{(0)} = 3 \times 10^{19} m^{-3}$, $R = 1.75m$, $a = 0.46m$, $r = 0.35m$, $B = 2.25T$, $A_i = 2$,

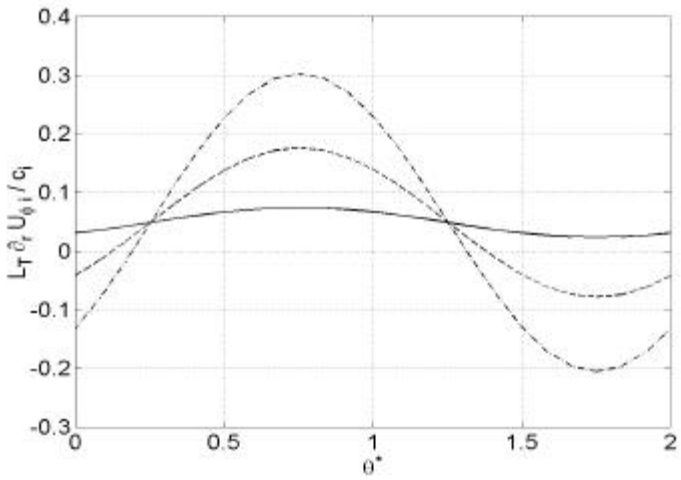

FIG.1. The plot of the normalized toroidal flow as a function of q^* *for* $\delta^{(0)} = 1.0\times10^{-5}$ *(solid line),* $\delta^{(0)} = 5.0\times10^{-5}$ *(dashed line),* $\delta^{(0)} = 1.0\times10^{-4}$ *(dashed-dotted line) and* $Z_{eff} = 1.5$.

$Z_{effi} = 1.5$. From the ion temperature profile [7] the value of $(-\partial \ln T_i / \partial r)^{-1} = L_{T_i} \sim 0.05m$ at $r = 0.35m$. In Fig. (1) we have plotted the normalized toroidal flow $[(L_{T_i}\left|-\partial U_{\phi,i}/\partial r\right|)/c_i]$ as a function of q^* for various values of $\delta^{(0)}$ and fixed a value of $Z_{eff} = 1.5$. This figure demonstrates that the toroidal flow may be significantly enhanced by the asymmetric radiation even if the asymmetric temperature perturbation is less than 0.1% (this corresponds to a radiation asymmetry parameter Δ_1 in the range of about ten per cent).

We now present a semi-quantitative explanation of how a small poloidal asymmetry in the radiated power could change the basic characteristic of L-mode discharges in a tokamak and then lead to a. L – RI mode transition. We follow the basic method used by Tokar [7] to study bifurcations of the tokamak plasma through the stationarity condition of the continuity equation describing the balance of sources and convective fluxes due to various components of the turbulence. We consider a simple case where the spatial symmetry breaking term due to $\vec{E}\times\vec{B}$ shear rotation reduces [20-21] the linear growth of the instabilities (i.e., ITG mode, DTE mode inside edge and DRBM in the outer edge of the plasma) and modifies stationarity condition in the continuity equation giving a new expression for the peaking factor [7]. In the presence of $\vec{E}\times\vec{B}$ shear rotation, the linear growth rate of the background instabilities have the general form $\gamma = \gamma^{\ln} - \gamma^{\ln}\Omega^2$, where $\gamma^{\ln}$ is the linear growth rate, the last term is the shear damping rate, Ω is the average radial symmetry breaking term [20, 22], $\Omega \equiv k_\theta U_E^{/} W_k / \gamma^{\ln}$, k_θ, and W_k are the poloidal wave vector, radial width of the instability.

We now derive the equation for peaking factor $p(=1/\eta_i)$, which comes from balancing the sources with the turbulent fluxes in the continuity equation. As stated earlier we assume that the ITG mode, DTE mode and the high-m DRBM dominate the transport inside the edge. The linear growth rates of these modes, without nonlinear damping, are well known and given as follows: (a) the ITG growth rate [11] has the form $\gamma^{ITG} = \gamma^{ITG} - \gamma^{ITG}\Omega^2$, $\gamma^{ITG} \cong \bar{\gamma}_0^{\,ITG} F(p)$, $F(p) = \sqrt{(1-0.17p-0.25\varepsilon_i p^2 - 1.36/\varepsilon_i)}$, $\bar{\gamma}_0^{\,ITG} = 2(k_\theta \rho_s c_s / R)\varepsilon_i^{1/2}$, $k_\theta \rho_s \approx 0.5$, and $\gamma^{\ln}\Omega^2 \equiv \gamma_{E\times B} \approx (<U_E>^{/})^2/\gamma^{\ln}$ is the flow shear damping rate, (b) DTE mode growth rate [7,12-13] $\gamma^{DTE} = 8(k_\theta \rho_s c_s / R)^2 (r\varepsilon_e \varepsilon_i / R\nu_e) f_{tr} (p - 0.5\hat{s}/\varepsilon_i\varepsilon)$ and $k_\theta \rho_s \approx 0.5$ (c) the linear growth rate of high-m DRBM $\approx c_s(\sqrt{2/RL_n})$ and $k_r^{-1} \approx (2\pi q\rho_s)^2 (R\nu_e / c_e)(m_e/m_i)^{1/2}\varepsilon_i^{1/2} p^{1/2}$ is the radial correlation length [14]. The particle transport due to these instabilities is estimated from

mixing length argument $D^{AN} \approx \gamma^{\ln} / k_\theta{}^2$. The equation for peaking factor p, which emerges by balancing the particle fluxes due to ITG, DTE and DRBM modes with the sources, is given as

$$G(p) = \Gamma_0[\frac{p}{\varepsilon_i{}^{1/2}}\{F(p) - \frac{\gamma_{E\times B}}{\bar{\gamma}_0{}^{ITG}}\}$$
$$+ 2(\frac{r}{R})^{3/2}\frac{\varepsilon_e c_s}{\nu_e R}(p - 0.5\frac{\hat{s}}{\varepsilon_i\varepsilon})(p - \frac{\gamma_{E\times B}}{\bar{\gamma}_0{}^{DTE}}) \qquad (21)$$
$$+ 2(\pi q)^2(\frac{m_e}{m_i})^{1/2}(\frac{R\nu_e}{c_e})p^{3/2}\{p^{1/2} - \frac{\gamma_{E\times B}}{\bar{\gamma}_0{}^{DRBM}}\}] - S_e = 0$$

where the first term corresponds to particle flux due to ITG mode, second denotes the reduction in flux due to flow shear damping, third term represents the flux due to dissipative trapped electron (DTE) mode, the last term represents the inward particle flux originating from the edge (i.e., $S_e \sim 2.5\times 10^{19}/m^2\cdot\sec$) [7], $\Gamma_0 = 8N_e c_s(\rho_s\varepsilon_i/R)^2$ and $k_\theta\rho_s \sim 0.5$ (assumed). If $\vec{E}\times\vec{B}$ stabilization is strong enough to completely stabilize any of three instabilities the contribution to the particle flux due to that instability is taken as zero.

Fig (2) gives a plot of $G(p)$ versus p for a fixed value of $Z_{eff} = 1.5$ and various values of the radiation asymmetry parameter Δ_1. It is noted that for low values of Δ_1, $G(p)$ goes to zero at 3 values of p including a low value; thus the discharge can come to a stable stationary state with a low peaking factor and stay there without any bifurcation. This is because we have chosen a value of Z_{eff} which is lower than that of Tokar [7] so that the bifurcations studied by him are not operative. As we increase the value of the radiation asymmetry parameter Δ_1, even for these lower values of Z_{eff}, the plasma can display bifurcations into a peaked density state when Δ_1 exceeds about 9 percent; in these cases there is only one real solution to the equation $G(p) = 0$ and that results in a relatively high value of p. The basic reason for the density peakedness is the considerably increased velocity shear at higher values of Δ_1 which strongly stabilizes the turbulence and hence requires higher values of density gradient for a balance of the weakened turbulent fluxes and the original sources in the continuity equation.

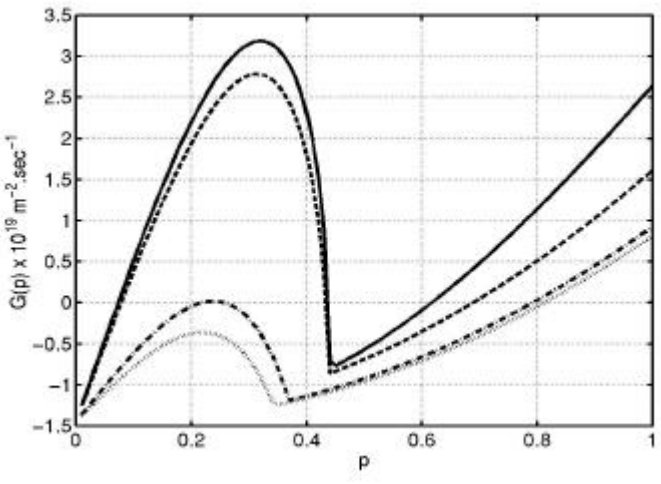

Fig. 2. Turbulent particle flux as a function of peaking parameter for various values of $\delta^{(0)} = 1.0\times 10^{-5}$ *(solid line),* $\delta^{(0)} = 1.0\times 10^{-4}$ *(dashed line),* $\delta^{(0)} = 3.7\times 10^{-4}$ *(dashed-dotted line),* $\delta^{(0)} = 4\times 10^{-4}$ *(dotted line).*

In conclusion, we have shown that small poloidal asymmetries in the radiation at the edge of an impurity seeded tokamak plasma can lead to significant sheared toroidal flow. These flows

contribute to the stabilization of edge instabilities and lead to the bifurcation of the plasma into an improved confinement mode viz. the RI mode. The bifurcation transition in the presence of poloidal asymmetries takes place at lower plasma dilutions than usual .We have carried out the calculations in the collisional neoclassical limit which are applicable to the outer 25% of the plasma where the radiative effects may be large. However, the sheared flow may extend to the plasma interior either through various possible pinch mechanisms of momentum transport e.g. see Ref. [22] or through inward propagation of a front with increased $\partial T_i / \partial r$ and $\partial E_r / \partial r$ as envisaged in Ref. [23].

[1]. E. A. Lazarus, J. D. Bell and C. E. Bush *et al*., J. Nucl. Mater. **121**, 61 (1984).
[2]. E. A. Lazarus, J. D. Bell and C. E. Bush *et al*., Nucl. Fusion **25**, 135 (1985).
[3]. A. M. Messiaen, J. Ongena, U. Samm *et al*., Phy. Rev. Lett. **77**, 2487 (1996).
[4]. R. Weynants, A. Messiaen, J. Ongena *et al*., Nucl. Fusion **39**, 1637 (1999).
[5]. J. Ongena, A. M. Messiaen *et al*., Plasma Phys. Control. Fusion **41**, A379 (1999).
[6]. G. Mank, A. M. Messiaen, J. Ongena *et al*., Phys. Rev. Lett. **85**, 2312 (2000).
[7]. M. Z. Tokar, J. Ongena, B. Unterberg *et al*., Phys. Rev. Lett. **84**, 895 (2000).
[8]. M. Z. Tokar, R. Jaspers, R. R. Weynants, H. R. Koslowski, et al., Plasma Physics Control Fusion **41**, L9 (1999); M. Z. Tokar, R. Jaspers, H. R. Koslowski, et al., Plasma Phys. Control Fusion **41**, B317 (1999);
[9]. R. D. Hezeltine, Phys. Fluids **17**, 961 (1974).
[10]. A. Claassen, H. Gerhauser, A. Rogister et al, Phys. Plasmas **7**, 3699 (2000).
[11]. Weiland, Collective Modes in Inhomogeneous Plasma (IOP Publishing Ltd, 2000), p. 132.
[12]. B. Kadomtsev and O. P. Pogutse, Nucl. Fusion **11**, 67 (1971).
[13]. Nilsson and J. Weiland, Nucl. Fusion **34**, 803 (1994).
[14]. S.V. Novakovskii et al., phys. Plasmas **2**, 781 (1995); P. N. Guzdar et al., Phys. Fluids B **5**, 3712 (1993); B. N. Rogers et al., Phys. Rev. Lett. **81**, 4396 (1998).
[15]. S. I. Braginskii, in Reviews of Plasma Physics, edited by M. A. Leontovich (consultants Bureau, New York, 1965), Vol. 1, P. 214.
[16]. M. Z. Tokar, Phys. Plasmas **6**, 2866 (2001).
[17]. A. B. Mikhailovskii and V. S. Tsypin, Sov. Phys. – JETP **56**, 75 (1982); A. B. Mikhailovskii and V. S. Tsypin, Zh. Eksp. Teor. Fiz **83**, 139 (1982).
[18]. A. Rogister, Phys. Plasmas **1**, 619 (1994).
[19]. R. Singh, A. Rogister and P. K. Kaw, Phys. Plasmas **11**, 129 (2004).
[20]. H. Biglari, P. H. Diamond and P. W. Terry, Phys. Fluids B **2**, 1 (1990).
[21]. T. S. Hahm and K. H. Burrel, Phys. Plasmas **2**, 1648 (1995).
[22]. B. A Carreras et al, Phys. Plasmas **1**, 4014 (1994).
[23]. A. L. Rogister, Nucl. Fusion **44**, 869 (2004).
[24]. A. L. Rogister, Nucl. Fusion **41**, 1101 (2002).